Evaluation of the Lagrangian Method for Deriving Equivalent Circuits of Integrated Magnetic Components: A Case Study Using the Integrated Winding Coupled Inductor

Kazuhiro Umetani,, Seikoh Arimura, Tetsuo Hirano
Advanced Semiconductor R&D
DENSO CORPORATION
500-1 Minamiyama, Komenoki-cho, Nisshin, Aichi, Japan

Jun Imaoka and Masayoshi Yamamoto
Interdisciplinary Faculty of Science and Engineering
Shimane University
1060 Nishikawatsu, Matsue, Shimane 690-8504, Japan

Published in: IEEE Transactions on Industry Applications
(Volume: 51 , Issue: 1 , Jan.-Feb. 2015)

DOI: 10.1109/TIA.2014.2330071

Evaluation of the Lagrangian Method for Deriving Equivalent Circuits of Integrated Magnetic Components: A Case Study Using the Integrated Winding Coupled Inductor

Kazuhiro Umetani, *Member, IEEE*, Jun Imaoka, *Student Member, IEEE*,
Masayoshi Yamamoto, *Member, IEEE*, Seikoh Arimura, and Tetsuo Hirano

***Abstract*—Recently Lagrangian dynamics has been applied to transforming integrated magnetic components into equivalent circuits of transformers and inductors. This Lagrangian method is expected to yield an equivalent circuit with few components, when applied to an integrated magnetic component with few flux paths that can be magnetized independently. However, properness of this method has not been verified. As a case study, this paper derives the equivalent circuit of the integrated winding coupled inductor using the Lagrangian method to evaluate consistency with the magnetic circuit model and experimental behavior. As a result, the Lagrangian method yielded a simpler equivalent circuit than those by the conventional methods. Additionally, the equivalent circuit of the Lagrangian method is found to be functionally equivalent to the magnetic circuit model and consistent with the experiment. These results support that the Lagrangian method provides proper equivalent circuits, and is useful for deriving simple equivalent circuits in some cases.**

***Index Terms*—Integrated magnetic components, Lagrangian, equivalent circuits, magnetic circuits.**

I. Introduction

A. Motivation

RECENT expansion of the application of power electronics in industry has intensified the need to miniaturize power converters. Consequently, circuit elements that constitute the power converters also need to be minimized. Miniaturizing magnetic components such as transformers and inductors is crucial in many cases, because they tend to occupy significant volume.

A possible remedy for the purpose is to employ integrated magnetic components [1]–[23]. These integrated components are composed of multiple windings on a single core, thus implementing the electric functions of plural basic magnetic components such as inductors and transformers. Integrating inductors and transformers possibly allows saving of space. In addition, in a well-designed structure, the windings possibly share the flux. This leads to reduction in the total amount of flux, thus enabling miniaturization of the core [2], [3], [19]. Magnetic coupling between windings may also enhance the electric functions. As a consequence, the total amount of copper used may also be reduced, as reported in [4], because a smaller number of turns may implement the same inductance. Owing to these benefits, a number of magnetic structures have been studied and reported [1]–[23].

However, the integrated magnetic components often have complex magnetic circuits, particularly if leakage flux paths are considered. Consequently, their electric functions can be difficult to comprehend, compared to a basic inductor or transformer with a single magnetic path. If power converters with integrated magnetic components are analyzed directly, both the electric and magnetic circuits must be handled simultaneously. Accordingly, such analysis tends to be complex compared to that only of electric circuits. Examples of this approach are presented in [1]-[4], [6], [13], [16] [18], [20].

This approach calculates all the flux in the magnetic circuit, and thus it is useful for precise design of the magnetic core dimension. Conversely, the complex analysis procedure may hinder intuitive comprehension of the overall circuit behavior. Consequently, the industrial applications of the integrated magnetic components may be promoted by developing methods that can easily analyze circuit behaviors.

B. Review of Preceding Approaches

One promising strategy is to express the electric functions of an integrated magnetic component as a functionally equivalent electric circuit composed of inductors and transformers [5], [10], [12], [19], [20], [21], [23]. Hereafter, we refer to this circuit as the equivalent circuit.

To the best of our knowledge, three methods to derive equivalent circuits have been proposed. These methods generally derive equivalent circuits that differ from others. Selecting a simpler equivalent circuit may therefore contribute to effortless circuit analysis.

The inductance matrix method [12] is one such method. This first identifies the leakage inductance of all windings, and the

Kazuhiro Umetani, Arimura Seikoh, and Tetuo Hirano are with DENSO CORPORATION, 1-1 Showa-cho, Kariya, Aichi Pref., 448-8661, Japan (e-mail: KAZUHIRO_Z_UMETANI@denso.co.jp).

Jun Imaoka and Masayoshi Yamamoto are with Interdisciplinary Faculty of Science and Engineering, Shimane University, 1060 Nishikawatsu, Matsue, Shimane Pref., 690-8504, Japan (e-mail: s139901@matsu.shimane-u.ac.jp, yamamoto@ecs.shimane-u.ac.jp).

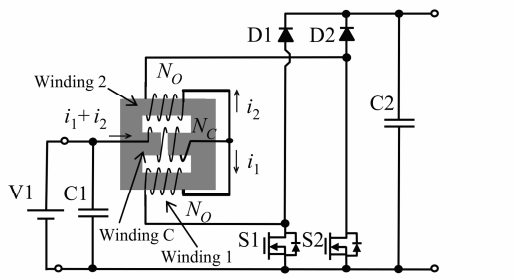

Fig. 1. Interleaved converter with the integrated winding coupled inductor.

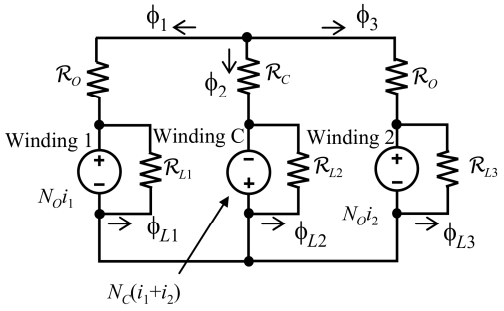

Fig. 2. Magnetic circuit model of the integrated winding coupled inductor.

mutual inductance [26] of all winding pairs. Each leakage inductance is then directly transformed into an inductor, and each of the mutual inductances into a transformer. Hence, the integrated magnetic component with n windings is generally expressed by an equivalent circuit with n inductors and $n(n-1)/2$ transformers.

The duality method has also been used [24] [25]. An advantage of this method is its straightforward derivation process. The method first transforms the network of the magnetic circuit model [27] of an integrated magnetic component. Specifically, the series-connections of the original network are transformed into parallel connections, and vice versa. Each reluctance is then replaced by an inductor, and all except one of the magnetomotive forces are replaced by an ideal transformer. The remaining magnetomotive force is eliminated. Consequently, if the integrated magnetic components contain n windings and m reluctance, the resultant equivalent circuit derived from the duality method will have $n-1$ transformers and m inductors.

The recently-proposed Lagrangian method [28] can also be used. This method is obtained by theoretical discussion on the Lagrangian dynamics of the integrated magnetic components, and utilizes Lagrangian expression for magnetic circuits. As discussed in [28, Sec. 3.2], the method transforms an integrated magnetic component into an equivalent circuit, composed of as many transformers and inductors as the flux paths of the original component that can be magnetized independently. This method can thus be expected to yield a simple equivalent circuit, if the integrated magnetic component has a small number of independent flux paths.

However, the properness of the equivalent circuit derived by this method has not been verified in the literature, although consistency of the method with Lagrangian dynamics suggests that it is proper [28].

C. Purpose of This Paper

To verify the Lagrangian method, this paper presents a case study using the integrated winding coupled inductor [4] [21]. The integrated winding coupled inductor has three windings. Its magnetic circuit model, as shown in this paper, has six reluctances, three magnetomotive forces, and five independent flux paths, including leakage flux paths. Consequently, among the three methods, the Lagrangian method is expected to yield the equivalent circuit with fewest magnetic components.

The following discussion is divided into four sections. Section II derives the equivalent circuits using the three methods to show that the Lagrangian method yields an equivalent circuit differing from those by the conventional methods, i.e. the inductance matrix method and the duality method. Section II also shows that the equivalent circuit from the Lagrangian method has fewest components, as expected.

Section III then shows theoretically that the equivalent circuit by the Lagrangian method is consistent with the magnetic circuit model, as are those by the conventional methods. For this purpose, we compare the electric functions of the equivalent circuits of the Lagrangian method and the inductance matrix method with the magnetic circuit model.

Section IV experimentally confirms that the equivalent circuits discussed in Section III are also consistent with experimental behavior of the integrated winding coupled inductor.

The conclusions are then presented in Section V.

II. Derivation of Equivalent Circuits

A. Integrated Winding Coupled Inductor

The interleaved converter with the integrated winding coupled inductor [4][21] is illustrated in Fig. 1. The magnetic core has three legs, each of which has a winding. Input current flows into winding C, and the current is then split into windings 1 and 2.

In this paper, we ignore non-linearity due to magnetic saturation or core loss. Similar to the conventional methods, the Lagrangian method also does not allow non-linearity so far, because it assumes linear media of the electromagnetic field.

The magnetic circuit model [27] of the integrated magnetic component can be expressed as in Fig. 2. We denote the electric current of windings 1 and 2 as i_1 and i_2, respectively. The outer legs and the center leg have windings with the number of turns N_O and N_C, and the reluctances $\mathcal{R}_O$ and $\mathcal{R}_C$, each of which are made by core and gaps. We assume that both outer legs have the same reluctance $\mathcal{R}_O$ and the number of turns N_O, according to the design concept of the magnetic structure. Leakage flux paths of the windings are implemented as the reluctance $\mathcal{R}_{L1}$–$\mathcal{R}_{L3}$.

B. Lagrangian Method

Based on Fig. 2, we derive an equivalent circuit according to the Lagrangian method proposed in [28]. The method provides

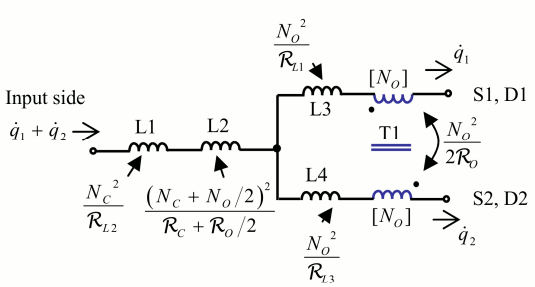

(a)

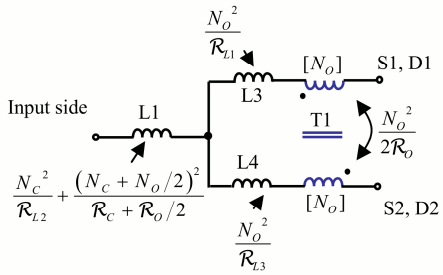

(b)

Fig. 3. Equivalent circuit by the Lagrangian method. (a) Direct translation from Lagrangian. (b) Simplified circuit with fewer inductors. Values in brackets are the number of turns. Values without brackets are the self-inductance for the inductors or the mutual inductance for the transformers.

Lagrangian expressions for an integrated magnetic component, which are directly configurable from their electric and magnetic network. We first translated Fig. 2 into Lagrangian. We then applied point transformation [29] to the result. Based on this, we obtained another Lagrangian belonging to an equivalent circuit. Finally, the equivalent circuit was obtained by translating the resultant Lagrangian into a physical circuit.

In the Lagrangian expression, the current flowing through a winding is regarded as the time derivative of the cumulative charge q [28], which is the time integration of the current i from the initial time t_0 to the time t:

$$q = \int_{t_0}^{t} i dt \,. \tag{1}$$

We denote the cumulative charge for i_1 and i_2 as q_1 and q_2, respectively. Translation of Fig. 2 yields the Lagrangian L:

$$\begin{aligned} L = & -N_O \dot{q}_1 (\phi_1 + \phi_{L1}) + N_C (\dot{q}_1 + \dot{q}_2)(\phi_2 + \phi_{L2}) \\ & - N_O \dot{q}_2 (\phi_3 + \phi_{L3}) - \mathcal{R}_{L1} \phi_{L1}^{\,2}/2 - \mathcal{R}_{L2} \phi_{L2}^{\,2}/2 \\ & - \mathcal{R}_{L3} \phi_{L3}^{\,2}/2 - \mathcal{R}_O \phi_1^{\,2}/2 - \mathcal{R}_C \phi_2^{\,2}/2 - \mathcal{R}_O \phi_3^{\,2}/2 \\ & + \lambda (\phi_1 + \phi_2 + \phi_3), \end{aligned} \tag{2}$$

where λ is a Lagrangian multiplier, and the dot over a variable is its time derivative.

The term with λ is eliminated by substituting $\phi_3 = -\phi_1 - \phi_2$ into (2). Additionally, we replace ϕ_1 by introducing

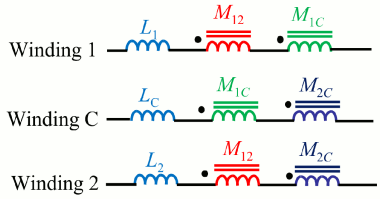

Fig. 4. Replacing each winding of the integrated winding coupled inductor by an inductor representing the leakage inductance and transformers representing the mutual inductance.

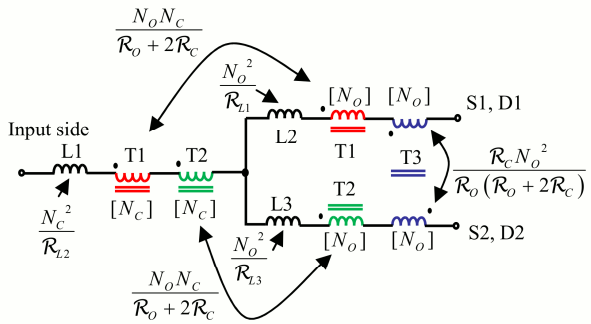

Fig. 5. Equivalent circuit by the inductance matrix method. Values in brackets are the number of turns. Values without brackets are the self-inductance for the inductors or the mutual inductance for the transformers.

$\phi_A = \phi_1 + \phi_2/2$. The purpose of introducing ϕ_A is to express the magnetic energy terms, i.e. the 4th–9th right-hand terms of (2), in the diagonal form of the fluxes without using the Lagrangian multiplier. Consequently, we obtain:

$$\begin{aligned} L = & (N_O \dot{q}_2 - N_O \dot{q}_1)\phi_A - \mathcal{R}_O \phi_A^{\,2} \\ & + (N_C + N_O/2)(\dot{q}_1 + \dot{q}_2)\phi_2 - (\mathcal{R}_C/2 + \mathcal{R}_O/4)\phi_2^{\,2} \\ & - N_O \dot{q}_1 \phi_{L1} - \mathcal{R}_{L1} \phi_{L1}^{\,2}/2 - N_O \dot{q}_2 \phi_{L3} - \mathcal{R}_{L3} \phi_{L3}^{\,2}/2 \\ & + N_C (\dot{q}_1 + \dot{q}_2)\phi_{L2} - \mathcal{R}_{L2} \phi_{L2}^{\,2}/2. \end{aligned} \tag{3}$$

Equation (3) corresponds to a circuit of transformers and inductors. Translating (3) yields the equivalent circuit shown in Fig. 3(a). Along with the circuit diagram, we also present the self and mutual inductance of the constituting elements.

The Lagrangian method preserves the number of independent fluxes. Note that ϕ_3 is dependent on ϕ_1 and ϕ_2, because the constraint $\phi_1 + \phi_2 + \phi_3 = 0$ is represented by the last right-hand term of (2). Hence, (2) contains five independent fluxes, namely ϕ_{L1}, ϕ_{L2}, ϕ_{L3}, ϕ_1, ϕ_2. Consequently, the resultant equivalent circuit is composed of five magnetic components, each of which consists of a single independent flux path.

Fortunately, in this case the equivalent circuit can be simplified further, because inductors L1 and L2 are connected in series. By replacing them by an inductor whose inductance is their sum, we obtain Fig. 3(b), which is composed of only four magnetic components. The result is similar to the equivalent circuit proposed in [4]. Nonetheless, our result is derived automatically under the predetermined procedure.

C. Inductance Matrix Method

In the inductance matrix method, the leakage and mutual inductance are calculated for each winding. The leakage inductance is transformed into an inductor with the same inductance, and the mutual inductance is transformed into a transformer with the same mutual inductance. Finally, the equivalent circuit is obtained by replacing each winding in the original component by a series-connection of the inductor and the transformers that represent the leakage and mutual inductance of the windings.

Now, we derive the equivalent circuit according to the inductance matrix method. To calculate the leakage and mutual inductance, we first solve the magnetic circuit model presented in Fig. 2. In the magnetic circuit, the flux follows Kirchhoff's current law, and the magnetomotive force follows Kirchhoff's voltage law. In calculation of the inductance, the method does not utilize the fact that the current of winding C is equal to the sum of windings 1 and 2. Therefore, we denote the current of the winding C as i_C. Hence, we have:

$$\begin{cases} \mathcal{R}_{L1}\phi_{L1} = -N_O i_1, \\ \mathcal{R}_{L2}\phi_{L2} = N_C i_C, \\ \mathcal{R}_{L3}\phi_{L3} = -N_O i_2, \\ \mathcal{R}_C\phi_2 - \mathcal{R}_O\phi_1 = N_C i_C + N_O i_1, \\ \mathcal{R}_C\phi_2 - \mathcal{R}_O\phi_3 = N_C i_C + N_O i_2, \\ \phi_1 + \phi_2 + \phi_3 = 0. \end{cases} \tag{4}$$

Solving the above equations with respect to the fluxes, we obtain:

$$\begin{aligned} &\phi_{L1} = -\frac{N_O}{\mathcal{R}_{L1}} i_1, \quad \phi_{L2} = \frac{N_C}{\mathcal{R}_{L2}} i_C, \quad \phi_{L3} = -\frac{N_O}{\mathcal{R}_{L3}} i_2, \\ &\phi_1 = -\frac{N_C}{\mathcal{R}_O + 2\mathcal{R}_C} i_C - \frac{(\mathcal{R}_O + \mathcal{R}_C) N_O}{\mathcal{R}_O (\mathcal{R}_O + 2\mathcal{R}_C)} i_1 \\ &\quad + \frac{\mathcal{R}_C N_O}{\mathcal{R}_O (\mathcal{R}_O + 2\mathcal{R}_C)} i_2, \\ &\phi_2 = \frac{2N_C}{\mathcal{R}_O + 2\mathcal{R}_C} i_C + \frac{N_O}{\mathcal{R}_O + 2\mathcal{R}_C}(i_1 + i_2), \\ &\phi_3 = -\frac{N_C}{\mathcal{R}_O + 2\mathcal{R}_C} i_C + \frac{\mathcal{R}_C N_O}{\mathcal{R}_O (\mathcal{R}_O + 2\mathcal{R}_C)} i_1 \\ &\quad - \frac{(\mathcal{R}_O + \mathcal{R}_C) N_O}{\mathcal{R}_O (\mathcal{R}_O + 2\mathcal{R}_C)} i_2. \end{aligned} \tag{5}$$

We denote the total flux that interlinks with windings 1, C, and 2 as ϕ_{T1}, ϕ_{TC}, and ϕ_{T2}, respectively. Using the above equation, ϕ_{T1}, ϕ_{TC}, and ϕ_{T2} can be expressed as:

$$\begin{aligned} \phi_{T1} &= -\frac{N_C}{\mathcal{R}_O + 2\mathcal{R}_C} i_C - \left\{ \frac{\mathcal{R}_O + \mathcal{R}_C}{\mathcal{R}_O (\mathcal{R}_O + 2\mathcal{R}_C)} + \frac{1}{\mathcal{R}_{L1}} \right\} N_O i_1 \\ &\quad + \frac{\mathcal{R}_C N_O}{\mathcal{R}_O (\mathcal{R}_O + 2\mathcal{R}_C)} i_2, \\ \phi_{TC} &= \left(\frac{2}{\mathcal{R}_O + 2\mathcal{R}_C} + \frac{1}{\mathcal{R}_{L2}} \right) N_C i_C + \frac{N_O}{\mathcal{R}_O + 2\mathcal{R}_C}(i_1 + i_2), \\ \phi_{T2} &= -\frac{N_C}{\mathcal{R}_O + 2\mathcal{R}_C} i_C + \frac{\mathcal{R}_C N_O}{\mathcal{R}_O (\mathcal{R}_O + 2\mathcal{R}_C)} i_1 \\ &\quad - \left\{ \frac{\mathcal{R}_O + \mathcal{R}_C}{\mathcal{R}_O (\mathcal{R}_O + 2\mathcal{R}_C)} + \frac{1}{\mathcal{R}_{L3}} \right\} N_O i_2. \end{aligned} \tag{6}$$

Next, we derive the inductance matrix. Electric functions of a magnetic component can be expressed as an inductance matrix. As for a magnetic component with three windings, the general definition of the matrix is expressed as:

$$\begin{pmatrix} V_1 \\ V_C \\ V_2 \end{pmatrix} = \begin{pmatrix} -N_O \dfrac{d\phi_{T1}}{dt} \\ N_C \dfrac{d\phi_{TC}}{dt} \\ -N_O \dfrac{d\phi_{T2}}{dt} \end{pmatrix} = \begin{bmatrix} \Lambda_1 & M_{1C} & M_{12} \\ M_{1C} & \Lambda_C & M_{2C} \\ M_{12} & M_{2C} & \Lambda_2 \end{bmatrix} \begin{pmatrix} \dfrac{di_1}{dt} \\ \dfrac{di_C}{dt} \\ \dfrac{di_2}{dt} \end{pmatrix}, \tag{7}$$

where V_1, V_C, and V_2 are the induced voltage of windings 1, C, and 2, respectively; Λ_1, Λ_C, and Λ_2 are the self-inductance; and M_{1C}, M_{2C}, and M_{12} are the mutual-inductance. Substituting (6) into (7), the elements of the matrix are determined as follows:

$$\begin{aligned} \Lambda_1 &= \left\{ \frac{\mathcal{R}_O + \mathcal{R}_C}{\mathcal{R}_O (\mathcal{R}_O + 2\mathcal{R}_C)} + \frac{1}{\mathcal{R}_{L1}} \right\} {N_O}^2, \\ \Lambda_C &= \left(\frac{2}{\mathcal{R}_O + 2\mathcal{R}_C} + \frac{1}{\mathcal{R}_{L2}} \right) {N_C}^2, \\ \Lambda_2 &= \left\{ \frac{\mathcal{R}_O + \mathcal{R}_C}{\mathcal{R}_O (\mathcal{R}_O + 2\mathcal{R}_C)} + \frac{1}{\mathcal{R}_{L3}} \right\} {N_O}^2, \\ M_{1C} &= M_{2C} = \frac{N_C N_O}{\mathcal{R}_O + 2\mathcal{R}_C}, \\ M_{12} &= -\frac{\mathcal{R}_C {N_O}^2}{\mathcal{R}_O (\mathcal{R}_O + 2\mathcal{R}_C)}. \end{aligned} \tag{8}$$

We seek a circuit that represents the same inductance matrix, by replacing each winding by a series connection of an inductor and two transformers, as shown in Fig. 4. We assume that each transformer represents the magnetic coupling of a winding pair, and its mutual inductance is equal to the matrix element that corresponds to the coupling. Furthermore, it is assumed that the transformers have the same number of turns as the original winding.

Note that the self-inductance of the original winding equals the sum of self-inductance of the inductor and transformers. In

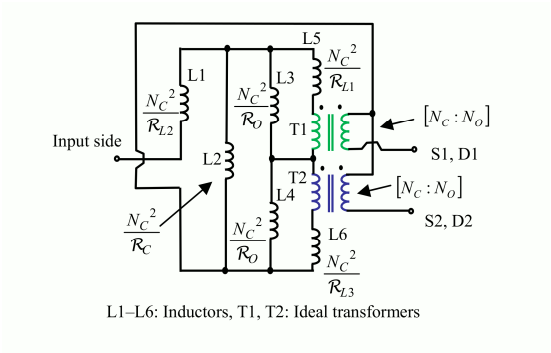

Fig. 6. Equivalent circuit by the duality method. Values in brackets are the ratios of the number of turns. Values without brackets are the self-inductance for the inductors.

other words, the self-inductance of the inductor corresponds to the leakage inductance [30] of the original winding. If the self-inductance of the inductors that replace windings 1, C, and 2 are denoted as L_1, L_C, and L_2, respectively, we obtain:

$$\begin{aligned} L_1 &= \Lambda_1 - M_{1C}\frac{N_O}{N_C} - M_{12}\frac{N_O}{N_O} = \frac{N_O{}^2}{\mathcal{R}_{L1}}, \\ L_C &= \Lambda_C - M_{1C}\frac{N_C}{N_O} - M_{2C}\frac{N_C}{N_O} = \frac{N_C{}^2}{\mathcal{R}_{L2}}, \\ L_2 &= \Lambda_2 - M_{2C}\frac{N_O}{N_C} - M_{12}\frac{N_O}{N_O} = \frac{N_O{}^2}{\mathcal{R}_{L3}}. \end{aligned} \tag{9}$$

Finally, we obtained the circuit illustrated in Fig. 5. Obviously, this is the equivalent circuit of the integrated winding coupled inductor. The equivalent circuit has three inductors, because the method yields as many inductors as the windings. It also has three transformers, which are as many as the winding pairs.

D. Duality Method

The detailed process of this method is presented in [24], [25]. We followed this process to derive the equivalent circuit for Fig. 2.

The duality method does not require calculation of the inductance matrix or translation of the magnetic circuit into Lagrangian expression. Instead, it requires the following two steps.

The first step is to transform the magnetic circuit network. In this transformation, each series-connection of the network is replaced by a parallel-connection, and vice versa.

The second step is to replace each element of the magnetic circuit model by an electric component. In this step, each reluctance is replaced by an inductor, and all except one magnetomotive forces are replaced by an ideal transformer. The remaining magnetomotive force is eliminated to extract a pair of terminals. The primary windings of the ideal transformers and the pair of terminals correspond to the windings of the original integrated magnetic component.

Consequently, the equivalent circuit for Fig. 2 is obtained as Fig. 6. The equivalent circuit contains six inductors, which is as many as the reluctance in Fig. 2. It contains two transformers, which equals the magnetomotive force less one.

E. Comparison between the Equivalent Circuits

As seen above, the three methods yield their own equivalent circuits, all of which differ. Compared to Fig. 5 and Fig. 6, Fig. 3(b) contains fewer magnetic components. In this case, the Lagrangian method thus yields simpler equivalent circuit. Hence, in some cases the Lagrangian method can be a helpful method for discussing the overall electric functions of an integrated magnetic component. For example, the Lagrangian method may possibly be useful in some cases when we invent a novel magnetic structure.

The main drawback of the Lagrangian method is that the voltage induced in the windings of the integrated magnetic component does not appear in the equivalent circuit, because generally a winding is not directly replaced by transformers and inductors. On the other hand, the equivalent circuits produced by the inductance matrix and duality methods directly present the induced voltage of any windings. The reason is that a winding is replaced by a series of connected inductors and transformers in the inductance matrix method, and by the primary winding of an ideal transformer or a pair of terminals in the duality method. Therefore, if it is necessary to discuss the induced voltage to design the insulation of the windings, the inductance matrix or duality methods seem preferable.

III. Analytical Equivalence of the Equivalent Circuits with the Magnetic Circuit Model

This section confirms that the equivalent circuit from the Lagrangian method has the same electric functions as the original magnetic circuit, similar to the equivalent circuits by the conventional inductance matrix and duality methods. For this purpose, we show that Fig. 3(a) is functionally equivalent to the original magnetic circuit, as well as Fig. 5. In order to discuss the functional equivalence, we employed the magnetic energy expressed as a function of current.

The electrical function of an integrated magnetic component can be fully determined if the magnetic energy $E(i_1, i_2, \ldots)$ is given as a function of the electric current. Here, we present a brief explanation of the reason.

We consider an arbitrary magnetic component with multiple current paths, and denote the voltage induced through the current path j as V_j. Because input energy equals the increase in magnetic energy, we have:

$$\sum_j V_j i_j = \sum_j \frac{\partial E}{\partial i_j}\frac{di_j}{dt}, \tag{10}$$

where i_j is the current of the current path j.

Because the magnetic energy is a quadratic form of the current, $\partial E/\partial i_j$ is a linear form of the current. By partially differentiating (10) with respect to the current, we obtain:

$$\begin{pmatrix} V_1 \\ V_2 \\ \vdots \end{pmatrix} = \begin{bmatrix} \dfrac{\partial E}{\partial i_1^{\,2}} & \dfrac{\partial E}{\partial i_1 \partial i_2} & \cdots \\ \dfrac{\partial E}{\partial i_2 \partial i_1} & \dfrac{\partial E}{\partial i_2^{\,2}} & \\ \vdots & & \ddots \end{bmatrix} \begin{pmatrix} \dfrac{di_1}{dt} \\ \dfrac{di_2}{dt} \\ \vdots \end{pmatrix}. \tag{11}$$

Equation (11) indicates that the energy expression $E(i_1, i_2, \ldots)$ is sufficient to determine the electrical input-output relation of the magnetic component. Hence, we only need to show that Fig. 3(b) and Fig. 5 belong to the same energy expression as that of the magnetic circuit model, in order to confirm the properness of the equivalent circuits.

First, we derive the energy expression for Fig. 2. The magnetic energy E_M of the whole magnetic circuit model is:

$$E_M = \frac{1}{2}\mathcal{R}_O\phi_1^{\,2} + \frac{1}{2}\mathcal{R}_C\phi_2^{\,2} + \frac{1}{2}\mathcal{R}_O\phi_3^{\,2} + \sum_{i=1}^{3}\frac{1}{2}\mathcal{R}_{Li}\phi_{Li}^{\,2}. \tag{12}$$

The energy expression for Fig. 2 is obtained by expressing the above equation as a function of i_1 and i_2. With a view to this purpose, the fluxes ϕ_1–ϕ_3 are expressed as functions of i_1 and i_2 in advance. Substituting i_C=i_1+i_2 into (5) yields:

$$\begin{aligned} \phi_1 &= -\frac{1}{2}\frac{N_O + 2N_C}{\mathcal{R}_O + 2\mathcal{R}_C}(i_1 + i_2) - \frac{1}{2}\frac{N_O}{\mathcal{R}_O}(i_1 - i_2), \\ \phi_2 &= \frac{N_O + 2N_C}{\mathcal{R}_O + 2\mathcal{R}_C}(i_1 + i_2), \\ \phi_3 &= -\frac{1}{2}\frac{N_O + 2N_C}{\mathcal{R}_O + 2\mathcal{R}_C}(i_1 + i_2) + \frac{1}{2}\frac{N_O}{\mathcal{R}_O}(i_1 - i_2). \end{aligned} \tag{13}$$

Substituting (5) and (13) into (12) leads to:

$$\begin{aligned} E_M = {} & \frac{1}{4}\mathcal{R}_O\left(\frac{N_O + 2N_C}{\mathcal{R}_O + 2\mathcal{R}_C}\right)^2 (i_1 + i_2)^2 \\ & + \frac{1}{4}\frac{N_O^{\,2}}{\mathcal{R}_O}(i_1 - i_2)^2 \\ & + \frac{1}{2}\mathcal{R}_C\left(\frac{N_O + 2N_C}{\mathcal{R}_O + 2\mathcal{R}_C}\right)^2 (i_1 + i_2)^2 \\ & + \frac{1}{2}\frac{N_O^{\,2}}{\mathcal{R}_{L1}}i_1^{\,2} + \frac{1}{2}\frac{N_C^{\,2}}{\mathcal{R}_{L2}}(i_1 + i_2)^2 + \frac{1}{2}\frac{N_O^{\,2}}{\mathcal{R}_{L3}}i_2^{\,2}. \end{aligned} \tag{14}$$

This is then compared with the energy expression for Fig. 3(b) and Fig. 5. The energy expression E_{Lag} for Fig. 3(b) is:

$$\begin{aligned} E_{Lag} = {} & \frac{1}{2}\left\{\frac{N_C^{\,2}}{\mathcal{R}_{L2}} + \frac{(N_C + N_O/2)^2}{\mathcal{R}_C + \mathcal{R}_O/2}\right\}(i_1 + i_2)^2 \\ & + \frac{1}{2}\frac{N_O^{\,2}}{2\mathcal{R}_O}(i_1 - i_2)^2 + \frac{1}{2}\frac{N_O^{\,2}}{\mathcal{R}_{L1}}i_1^{\,2} + \frac{1}{2}\frac{N_O^{\,2}}{\mathcal{R}_{L3}}i_2^{\,2}. \end{aligned} \tag{15}$$

TABLE I
SPECIFICATIONS OF THE PROTOTYPE CONVERTER

PARAMETER	Value
Input voltage V1	20–180 V
Output voltage (The voltage of C2)	200 V
Duty Ratio	0.1–0.9
Switching Frequency	50kHz
Semiconductor Devices (S1, S2, D1, D2)	MG50J1ZS40 (IGBT+Diode)
Decoupling Capacitors (C1, C2)	3300μF (Electrolytic Capacitor)
Winding Turn Number (N_C, N_O)	13 Turns
Reluctance R_C	14.4 A/μWb
Reluctance R_O	0.192 A/μWb
Reluctance R_{L1}	8.83 A/μWb
Reluctance R_{L2}	169 A/μWb
Reluctance R_{L3}	9.06 A/μWb

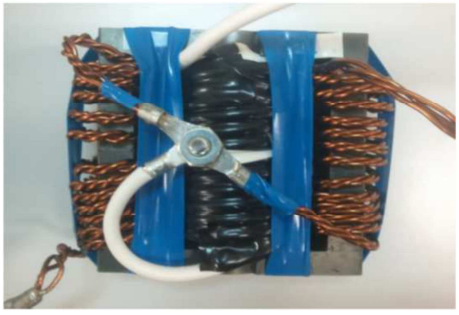

Fig. 7. Photograph of the integrated winding coupled inductor employed for the prototype converter.

On the other hand, the energy expression E_{Matrix} for Fig. 5 is:

$$\begin{aligned} E_{Matrix} = {} & \frac{1}{2}\frac{N_C^{\,2}}{\mathcal{R}_{L2}}(i_1 + i_2)^2 \\ & + \frac{1}{2}\frac{1}{\mathcal{R}_O + 2\mathcal{R}_C}(N_C i_1 + N_C i_2 + N_O i_1)^2 \\ & + \frac{1}{2}\frac{1}{\mathcal{R}_O + 2\mathcal{R}_C}(N_C i_1 + N_C i_2 + N_O i_2)^2 \\ & + \frac{1}{2}\frac{N_O^{\,2}}{\mathcal{R}_{L1}}i_1^{\,2} + \frac{1}{2}\frac{N_O^{\,2}}{\mathcal{R}_{L3}}i_2^{\,2} \\ & + \frac{1}{2}\frac{\mathcal{R}_C N_O^{\,2}}{\mathcal{R}_O(\mathcal{R}_O + 2\mathcal{R}_C)}(i_1 - i_2)^2. \end{aligned} \tag{16}$$

Equations (14)–(16) can be developed to obtain E_M=E_{Lag}=E_{Matrix}. Consequently, both Fig. 3(b) and Fig. 5 are shown to have the same electric functions as the magnetic circuit model.

IV. CONSISTENCY WITH EXPERIMENTAL BEHAVIOR

This section confirms consistency of the equivalent circuits with experimental behavior of the integrated magnetic

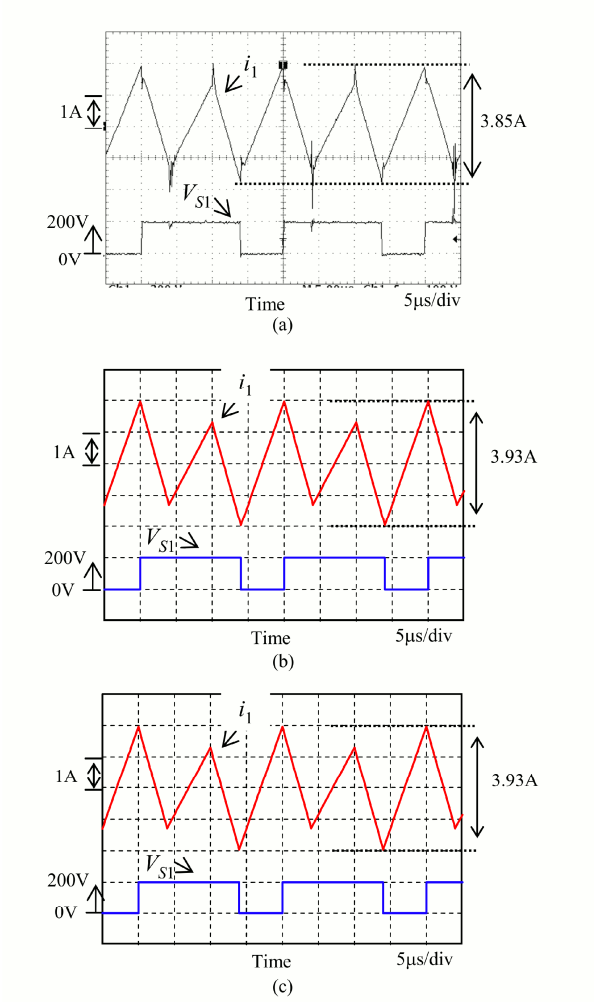

Fig. 8. Experimental and simulated waveforms of the current of the winding 1 (i_1) and the voltage across S1 (V_{S1}). (a) Experiment. (b) Simulation based on the Lagrangian method. (c) Simulation based on the inductance matrix method.

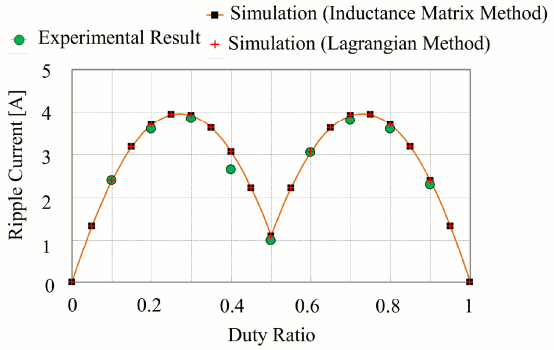

Fig. 9. Experimental and simulated ripple current in the current of the winding 1 (i_1)

component. Current waveforms of the converter shown in Fig. 1 were simulated utilizing the equivalent circuit shown in Fig. 3(b) and Fig. 5. The results were then compared with the experimental waveforms of a prototype converter with the integrated magnetic component. We employed SCAT K.460PR1 (Keisoku Giken Co., Ltd.) as the simulator.

The specifications of the prototype are given in Table 1, and a photograph of the magnetic component in Fig. 7. To simplify the waveform, the converter was operated under the continuous conduction mode. Hence, $\mathcal{R}_O$ is designed to be far smaller than the design concept presented in [4]. We equipped no gap on the outer legs. The reluctance of the magnetic circuit is estimated from results of inductance measurement of the magnetic component. Details of the estimation are presented in the appendix.

First, we compared the experimental and simulated waveform of the current i_1, when the duty ratio is set at 0.3. The result is shown in Fig. 8. Figure 8(a) is the experimental waveform, and Fig. 8(b) and Fig. 8(c) are the simulated waveforms of the equivalent circuits by the Lagrangian method and the inductance matrix method, respectively. The two simulated waveforms are identical, indicating equivalency between the two equivalent circuits, as expected from the previous section. In addition, the simulation predicted the experimental waveform well, except for surge current during the switching of S1 and S2.

Next, we compared the simulated current ripple of i_1 with the experimental result over several duty ratios. The result is shown in Fig. 9. As expected from the previous section, the simulation of the two equivalent circuits resulted in the same current ripple. In addition, the simulation successfully predicted dependency of the ripple current on duty ratio. Hence, the result also supported consistency of the equivalent circuit with the experiment. Certainly, the experiment showed that the ripple current was slightly smaller than predicted when the duty ratio was set at 0.4. The reason for this is not clear. However, the surge current during switching of S1 and S2 may have caused measurement deviation of the ripple current.

Consequently, we concluded that the experiment also supported the properness of the equivalent circuits.

V. Conclusion

Lagrangian dynamics have recently been applied to deriving the equivalent circuit of an integrated magnetic component. This method is expected to derive a simpler circuit than the conventional inductance matrix and duality methods, when applied to an integrated magnetic component with few flux paths that can be magnetized independently. However, the properness of the equivalent circuit by the Lagrangian method has not been verified.

As a case study, this paper investigated equivalent circuits of the integrated winding coupled inductor. The equivalent circuits were derived using the Lagrangian, inductance matrix, and duality methods, respectively. Among these three methods, the Lagrangian method yielded the equivalent circuit with fewest components. Specifically, the equivalent circuit by the Lagrangian method is composed of only four magnetic components.

We then investigated the consistency of the equivalent circuit by the Lagrangian method with the magnetic circuit model, and the experimental behavior of the integrated winding

coupled inductor. The results showed the equivalent circuit was functionally equivalent to the magnetic circuit model, and predicted the experimental behavior as well as the equivalent circuit produced by the inductance matrix method.

Consequently, these results support that the Lagrangian method provides proper equivalent circuits, and in some cases is useful for deriving simple equivalent circuits.

APPENDIX

The reluctance of the prototype of the integrated winding coupled inductor was estimated based on measurement of the self-inductance of all windings, and the mutual inductance of all winding pairs. The self-inductance is the inductance of a winding when all the other windings are opened. The result of the measurements is presented in Table II.

We can analytically express the inductance as functions of the reluctance. By equating the expression to the measured inductance, the reluctance can be determined.

The expression for the self and mutual inductance are already obtained in (8) by the inductance matrix method. However, this does not indicate that the inductance matrix method is more useful than the Lagrangian method, because we can also derive the same result by the latter. In order to prove this, we here employ the Lagrangian method to derive the expression.

We consider that the windings in Fig. 2 are disconnected each from the other. Then, Lagrangian L' of Fig. 2 can be described introducing q_C, which is the cumulative charge through the winding C:

$$\begin{aligned} L' = &-N_O\dot{q}_1(\phi_1+\phi_{L1})+N_C\dot{q}_C(\phi_2+\phi_{L2}) \\ &-N_O\dot{q}_2(\phi_3+\phi_{L3})-\mathcal{R}_{L1}{\phi_{L1}}^2/2-\mathcal{R}_{L2}{\phi_{L2}}^2/2 \\ &-\mathcal{R}_{L3}{\phi_{L3}}^2/2-\mathcal{R}_O{\phi_1}^2/2-\mathcal{R}_C{\phi_2}^2/2-\mathcal{R}_O{\phi_3}^2/2 \\ &+\lambda(\phi_1+\phi_2+\phi_3). \end{aligned} \tag{17}$$

We simplify (17) by eliminating λ and introducing $\phi_A=\phi_1+\phi_2/2$. Then, we have:

$$\begin{aligned} L' = &-N_O\dot{q}_1(\phi_A-\phi_2/2+\phi_{L1})+N_C\dot{q}_C(\phi_2+\phi_{L2}) \\ &-N_O\dot{q}_2(-\phi_A-\phi_2/2+\phi_{L3})-\mathcal{R}_{L1}{\phi_{L1}}^2/2 \\ &-\mathcal{R}_{L2}{\phi_{L2}}^2/2-\mathcal{R}_{L3}{\phi_{L3}}^2/2-\mathcal{R}_O{\phi_A}^2 \\ &-(\mathcal{R}_C/2+\mathcal{R}_O/4){\phi_2}^2. \end{aligned} \tag{18}$$

First, we determine the mutual inductance M_{1C} between the windings 1 and C. By substituting q_2=0, we can obtain the equivalent circuit of the magnetic component, when the winding 2 is opened:

$$\begin{aligned} L' = &-N_O\dot{q}_1(\phi_A-\phi_2/2+\phi_{L1})+N_C\dot{q}_C(\phi_2+\phi_{L2}) \\ &-\mathcal{R}_{L1}{\phi_{L1}}^2/2-\mathcal{R}_{L2}{\phi_{L2}}^2/2-\mathcal{R}_{L3}{\phi_{L3}}^2/2-\mathcal{R}_O{\phi_A}^2 \\ &-(\mathcal{R}_C/2+\mathcal{R}_O/4){\phi_2}^2. \end{aligned} \tag{19}$$

Now, we consider Lagrangian L_{temp} of an arbitrary circuit with the magnetic component represented by (19). In other words, L_{temp} contains the above Lagrangian L'. Because L_{temp} does not contain ϕ_{L3} except L', the Euler-Lagrange equation [26] of L_{temp} with respect to ϕ_{L3} gives ϕ_{L3}=0. Therefore, we can eliminate ϕ_{L3} from (19), obtaining:

$$\begin{aligned} L' = &-N_O\dot{q}_1\phi_A-\mathcal{R}_O{\phi_A}^2-N_O\dot{q}_1\phi_{L1}-\mathcal{R}_{L1}{\phi_{L1}}^2/2 \\ &+N_C\dot{q}_C\phi_{L2}-\mathcal{R}_{L2}{\phi_{L2}}^2/2 \\ &+(N_O\dot{q}_1/2+N_C\dot{q}_C)\phi_2-(\mathcal{R}_C/2+\mathcal{R}_O/4){\phi_2}^2. \end{aligned} \tag{20}$$

The above Lagrangian can be translated into Fig. 10(a). Therefore, the mutual inductance M_{1C} is:

$$M_{1C}=\frac{N_ON_C}{\mathcal{R}_O+2\mathcal{R}_C}. \tag{21}$$

Next, the self-inductance Λ_1 of winding 1 is obtained by further opening winding C. Substituting q_C=0 into (20) yields:

$$\begin{aligned} L' = &-N_O\dot{q}_1\phi_{L1}-\mathcal{R}_{L1}{\phi_{L1}}^2/2-N_O\dot{q}_1\phi_A-\mathcal{R}_O{\phi_A}^2 \\ &+N_O\dot{q}_1\phi_2/2-(\mathcal{R}_C/2+\mathcal{R}_O/4){\phi_2}^2. \end{aligned} \tag{22}$$

We eliminated the term with ϕ_{L2} in (22), because the Euler-Lagrange equation with respect to ϕ_{L2} now yields ϕ_{L2}= 0.

TABLE II
MEASUREMENT RESULT OF SELF- AND MUTUAL INDUCTANCE

PARAMETER	Value
Self-inductance of the winding 1 (Λ_1)	462 μH
Self-inductance of the winding C (Λ_C)	12.7 μH
Self-inductance of the winding 2 (Λ_2)	461.5 μH
Mutual-inductance between the windings 1 and C (M_{1C})	5.85 μH
Mutual-inductance between the windings 1 and 2 (M_{12})	437 μH
Mutual-inductance between the windings 2 and C (M_{2C})	5.85 μH

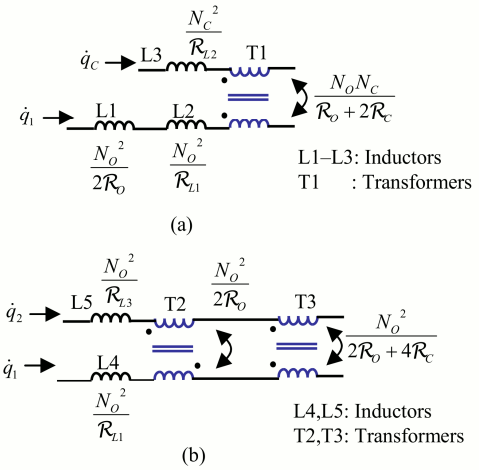

Fig. 10. Translation from Lagrangian expression into circuit diagram. (a) Equation (19). (b) Equation (25).

Equation (22) corresponds to series-connected inductors whose inductances are $N_O^2/\mathcal{R}_{L1}$, $N_O^2/2\mathcal{R}_O$, and $N_O^2/(2\mathcal{R}_O+4\mathcal{R}_C)$, respectively. Therefore, we have:

$$\Lambda_1 = \frac{N_O^{\ 2}}{\mathcal{R}_{L1}} + \frac{N_O^{\ 2}}{2\mathcal{R}_O} + \frac{N_O^{\ 2}}{2\mathcal{R}_O + 4\mathcal{R}_C}. \tag{23}$$

Similarly, the self-inductance Λ_C of winding C is obtained by substituting q_1=0 into (20). Then, ϕ_{L1}=0 and ϕ_A=0 can be substituted, according to the similar reason described above. As a result, we have:

$$\begin{aligned} L' &= N_C \dot{q}_C \phi_{L2} - \mathcal{R}_{L2} \phi_{L2}^{\ 2}/2 \\ &\quad + N_C \dot{q}_C \phi_2 - \left(\mathcal{R}_C/2 + \mathcal{R}_O/4\right)\phi_2^{\ 2}. \end{aligned} \tag{24}$$

Equation (24) corresponds to series connected inductors whose inductances are $N_C^2/\mathcal{R}_{L2}$ and $2N_C^2/(\mathcal{R}_O+2\mathcal{R}_C)$. Hence, we have:

$$\Lambda_C = \frac{N_C^{\ 2}}{\mathcal{R}_{L2}} + \frac{2N_C^{\ 2}}{\mathcal{R}_O + 2\mathcal{R}_C}. \tag{25}$$

Then, we determine the mutual inductance M_{12} between windings 1 and 2. Now, only winding C is opened. Thus, substitute q_C=0 into (18) to obtain:

$$\begin{aligned} L' &= -N_O \dot{q}_1 \phi_{L1} - \mathcal{R}_{L1} \phi_{L1}^{\ 2}/2 - N_O \dot{q}_2 \phi_{L3} - \mathcal{R}_{L3} \phi_{L3}^{\ 2}/2 \\ &\quad + \left(N_O \dot{q}_2 - N_O \dot{q}_1\right)\phi_A - \mathcal{R}_O \phi_A^{\ 2} \\ &\quad + \left(N_O \dot{q}_1 + N_O \dot{q}_2\right)\phi_2/2 - \left(\mathcal{R}_C/2 + \mathcal{R}_O/4\right)\phi_2^{\ 2}. \end{aligned} \tag{26}$$

Note that we eliminated the term with ϕ_{L2}, similarly as in (22). Equation (26) can be translated into Fig. 10(b). Therefore, the mutual inductance M_{12} is:

$$M_{12} = \frac{\mathcal{R}_C N_O^{\ 2}}{\mathcal{R}_O\left(\mathcal{R}_O + 2\mathcal{R}_C\right)}. \tag{27}$$

According to similar discussion to obtain (21) and (23), we obtain the self-inductance Λ_2 of winding 2 and the mutual inductance M_{2C} between windings 2 and C:

$$\Lambda_2 = \frac{N_O^{\ 2}}{\mathcal{R}_{L3}} + \frac{N_O^{\ 2}}{2\mathcal{R}_O} + \frac{N_O^{\ 2}}{2\mathcal{R}_O + 4\mathcal{R}_C}, \tag{28}$$

$$M_{2C} = \frac{N_O N_C}{\mathcal{R}_O + 2\mathcal{R}_C}. \tag{29}$$

Finally, the reluctance can be determined by equating Table 2 with (21), (23), (25), (27)–(29), obtaining the values of reluctance shown in Table 1.

REFERENCES

[1] D. K.-W. Cheng, Leung-Pong Wong, and Y.-S. Lee, "Design, modeling, and analysis of integrated magnetics for power converters," in *Proc. Power Electronics Specialists Conf.*, 2000, vol. 1, pp. 320-325.

[2] P. Zumel, O. Garcia, J. A. Cobos, and J. Uceda, "Magnetic integration for interleaved converters," in *Proc. Appl. Power Electron. Conf. and Expo.*, 2003, vol. 2, pp. 1143-1149.

[3] S. Chandrasekaran and L. U. Gokdere, "Integrated magnetics for interleaved DC-DC boost converter for fuel cell powered vehicles," in *Proc. Power Electronics Specialists Conf.*, 2004, pp. 356-361.

[4] Wei Wen, and Y.-S. Lee, "A two-channel interleaved boost converter with reduced core loss and copper loss," in *Proc. Power Electronics Specialists Conf.*, 2004, pp. 1003-1009.

[5] Leung-Pong Wong, Y. S. Lee, D. K. W. Cheng, and M. H. L. Chow, "Two-phase forward converter using an integrated magnetic component," *IEEE Trans. Aerosp. Electron. Syst.*, vol. 40, no. 4, pp. 1294-1310, Oct. 2004.

[6] L. Yan, and B. Lehman, "An integrated magnetic isolated two-inductor boost converter: analysis, design and experimentation," *IEEE Trans. Power Electron.*, vol. 20, no. 2, pp. 332-342, Mar. 2005.

[7] E. Laboure, A. Cuniere, T. A. Meynard, F. Forest, and E. Sarraute, "A theoretical approach to intercell transformers, application to interleaved converters," *IEEE Trans. Power Electron.*, vol. 23, no. 1, pp. 464-474, Jan. 2008

[8] L. P. Wong, Y. S. Lee, M. H. L. Chow, and D. K. W. Cheng, "A four-phase forward converter using an integrated transformer," *IEEE Trans. Ind. Electron.*, vol. 55, no. 2, pp.817-831, Feb. 2008.

[9] J. Sun and V. Mehrotra, "Orthogonal winding structures and design for planar integrated magnetics," *IEEE Trans. Ind. Electron.*, vol. 55, no. 3, pp. 1463-1469, Mar. 2008.

[10] T. Kawashima, S. Funabiki, and M. Yamamoto, "Recovery-less boost converter for electric vehicle," in *Proc. European Conf. Power Electron. and Applicat.*, 2009, pp. 1-10.

[11] J. Salmon, J. Ewanchuk, and A. M. Knight, "PWM inverters using split-wound coupled inductors," *IEEE Trans. Ind. Appl.*, vol. 45, no. 6, pp. 2001-2008, Nov./Dec. 2009.

[12] M. Nakahama, M. Yamamoto, and Y. Satake, "Trans-linked multi-phase boost converter for electric vehicle," in *Proc. Energy Conversion Congr. and Expo.*, 2010, Atlanta, pp. 2458-2463.

[13] H. N. Nagaraja, D. Kastha, and A. Patra, "Design principles of a symmetrically coupled inductor structure for multiphase synchronous buck converters," *IEEE Trans. Ind. Electron.*, vol. 58, no. 3, pp. 988-997, Mar. 2011.

[14] S. Roy and L. Umanand, "Integrated magnetics-based multisource quality AC power supply," *IEEE Trans. Ind. Electron.*, vol. 58, no. 4, pp. 1350-1358, April 2011.

[15] F. Yang, X. Ruan, Y. Yang, and Z. Ye, "Interleaved critical current mode boost PFC converter with coupled inductor," *IEEE Trans. Power Electron.*, vol. 26, no. 9, pp. 2404-2413, Sept. 2011.

[16] Z. Ouyang, Z. Zhang, O. C. Thomson, and M. A. E. Andersen, "Planar-integrated magnetics (PIM) module in hybrid bidirectional DC-DC converter for fuel cell application," *IEEE Trans. Power Electron.*, vol. 26, no. 11, pp. 3254-3264, Nov. 2011.

[17] S. Utz and J. Pforr, "Operation of multi-phase with coupled inductors at reduced numbers of phases," in *Proc. 14th European Conf. Power Electron. Applicat. (EPE)*, 2011, pp. 1-10.

[18] N. Zhu, J. Kang, D. Xu, B. Wu, and Y. Xiao, "An integrated AC choke design for common-mode current suppression in neural-connected power converter systems," *IEEE Trans. Power Electron.*, vol. 27, no. 3, pp. 1228-1236, Mar. 2012.

[19] W. Li, P. Li, H. Yang, and X. He, "Three-level forward-flyback phase-shift ZVS converter with integrated series-connected coupled inductors," *IEEE Trans. Power Electron.*, vol. 27, no. 6, pp. 2846-2856, Jun. 2012.

[20] D. O. Boillat and J. W. Kolar, "Modeling and experimental analysis of a coupled inductor employed in a high performance AC power source," in *Proc. Intl. Conf. Renewable Energy Research Applicat. (ICRERA)*, 2012, pp. 1-18.

[21] J. Imaoka, M. Yamamoto, K. Umetani, S. Arimura, and T. Hirano, "Characteristics analysis and performance evaluation for interleaved boost converter with integrated winding coupled inductor," in *Proc. Energy Conversion Congr. Expo.*, 2013, pp. 3711-3718.

[22] K. J. Hartnett, J. G. Hayes, M. G. Egan, and M. S. Rylko, "CCTT-core split-winding integrated magnetic for high-power DC-DC converters," *IEEE Trans. Power Electron.*, vol. 28, no. 11, pp. 4970-4984, Nov. 2013.
[23] C. Deng, D. Xu, P. Chen, C. Hu, W. Zhang, Z. Wen, and X. Wu, "Integration of both EMI filter and boost inductor for 1kW PFC converter," *IEEE Trans. Power Electron.*, vol. PP, issue 99, pp. 1, 2014.
[24] S. A. El-Hamamsy and E. I. Chang, "Magnetics modeling for computer-aided design of power electroncs circuits," in *Proc. Power Electron. Specialist Conf. (PESC)*, 1989, vol. 2, pp. 635-645.
[25] G. W. Ludwig and S. A. El-Hamamsy, "Coupled inductor and reluctance models of magnetic components," *IEEE Trans. Power Electron.*, vol. 6, no. 2, pp. 240-250, April 1991.
[26] J. D. Kraus, "Time changing electric and magnetic field," in *Electromagnetics*, 4th ed., New York: McGraw-Hill, 1991, pp. 432-435
[27] S. V. Marshall, and G. G. Skitek, "Magnetic circuits," in *Electromagnetic concepts and applications*, 3rd ed., New Jersey: Prentice Hall, 1990, pp. 276-283.
[28] K. Umetani, "A generalized method for Lagrangian modeling of power conversion circuit with integrated magnetic components," *IEEJ Trans. Elec. and Electron. Eng.*, vol. 7, issue S1, pp. S146-S152, Dec. 2012
[29] L. D. Landau, and E. M. Lifshitz, "Canonical transformations," in *Mechanics*, Oxford, U. K.: Butterworth-Heinemann, 1976, pp.143-146.
[30] A. Van den Bossche, and V. C. Valchev, "Fundamentals of magnetic theory," in *Inductors and transformers for power electronics*, Florida: CRC Press, 2005, pp. 17-29.

Kazuhiro Umetani (M'11) was born in Kobe, Japan, in 1980. He received a Ph.D degree in geophysical fluid dynamics from Kyoto University, Japan, in 2007.

He was a circuit design engineer at Toshiba Corporation, Japan, from 2007 to 2008.

Dr. Umetani is currently with the power group in DENSO CORPORATION, Japan. His research interests include new circuit configurations in power electronics and power magnetics for vehicular applications.

Jun Imaoka (M'11) received B.Sc. and M.Sc. degrees in electrical and electronic systems engineering from Shimane University, Shimane, Japan, in 2011 and 2013 respectively. He is currently working toward a Ph.D. degree in electrical and electronic systems engineering at Shimane University, Shimane, Japan. His research interests include design of magnetic components and modeling for high power density DC/DC converters and AC/DC converters.

Masayoshi Yamamoto (M'11) received M.S. and Ph.D. degrees in science and engineering from Yamaguchi University, Yamaguchi, Japan in 2000 and 2004, respectively. From 2004, he was with Sanken Electric Co., Ltd., Saitama, Japan. Since 2006, he has been with Shimane University, Shimane, Japan. His research interests include power supplies for HEV (boost converter, buck converter, 3-phase inverter, digital control), charging system for EV, LED illumination systems for tunnels, EMI of switching power supply, and wireless power transfer.

Seikoh Arimura received M.S. and Ph.D. degrees in Astrophysics from Nagoya University, in 1999 and 2003, respectively. From 2003 to 2005, he was a research assistant with the Japan Aerospace Exploration Agency (JAXA). Since 2005, he has been with DENSO CORPORATION, Aichi, Japan. His research interests include power electronics for boost converter and inverter in HV/EV system.

Tetsuo Hirano was born in Hamamatsu, Japan, in 1960. He received the M.S. degree in electronic engineering at Shizuoka University, Japan.

Since 1984, he has been with DENSO CORPORATION, Japan. His research interests include semiconductor circuit topologies and power electronics for vehicular applications.